JMEPEG (2011) 20:24–30
DOI: 10.1007/s11665-010-9642-0

1059-9495/$19.00

Enhancement of Surface Flashover Performance of High Voltage Ceramic Disc Insulators

B. Subba Reddy and Udaya Kumar

(Submitted September 18, 2009; in revised form February 7, 2010)

In this paper, an effort is made to study accurately the field distribution for various types of ceramic insulators used for high-voltage transmission. The surface charge simulation method (SCSM) is employed for the field computation. With the help of SCSM program, a Novel field reduction electrode is designed and developed to reduce the maximum field around the pin region. In order to experimentally analyze the performance of discs with field reduction electrode, special artificial pollution test facility was built and utilized. The experimental results show better surface flashover performance of ceramic insulators used in high-voltage transmission and distribution systems.

Keywords ceramic insulators, field reduction electrode, flashover

1. Introduction

Since the earliest days of power transmission and distribution, contamination flashover has inundated overhead lines. Flashover triggered by early morning dew/fog deposits were noted as early as in 1902, but the systematic research on pollution started in 1907 (Ref 1).

The adoption of higher transmission voltages after World War II motivated new interest in the problem. More recently, the realization that contamination on insulators may pose a fundamental threat to economical extra high voltage (EHV), and ultra high voltage (UHV) transmission has spawned numerous research projects throughout the world.

A major impact of the problem is that it can repeatedly occur even at working voltages. Because of these factors, a great deal of effort has already gone into to understand, as well as, model the same. Despite best efforts, success has only been nominal in improving the performance insulators used for high-voltage transmission/distribution under contaminated conditions.

It is worth mentioning that the failure at any single point of the transmission network can bring down the entire system. Recent reports (Ref 2, 3) on grid disturbance in India indicate the loss of 5000 million rupees and 97% of interconnected generation on January 2, 2001. Similar disturbances of lesser magnitudes were also observed during the period of December 2002 and 2005, February and December 2006, January and February 2007, and March 2008. One of the major causes identified was the pollution-/contamination-induced flashovers. These events have amply portrayed that the performance of overhead transmission line string insulators and that used in outdoor substations is a critical factor which governs the reliability of power delivery systems.

Motivated by this, the current study was undertaken and it essentially aims to seek simple alternative solutions for the problem. An interrogative study (Ref 4-6) on the problem has shown that the maximum electric field occurring on the surface near the pin and cap, especially the former, could be the accelerating source for pollution/contamination-induced flashover. However, a reliable electric field distribution data on commonly used disc insulators are rather inadequate. In fact, the field concentration near the pin can lead to early formation of dry band and scintillation/partial arcs. Considering this, it is intended in this work to seek possible minimization of the maximum field occurring at the surface near the pin region. This is expected to yield enhanced pollution/contamination flashover strength and in addition, improve wet flashover strength, as well as, reduction in audible and radio noise levels.

For obtaining the prevailing fields, suitable electric field computation tool is required. As the present problem under investigation is of open-geometry type and having multiple dielectrics, it is impractical to employ analytical methods as the geometry does not fit into orthogonal curvilinear coordinates. Hence, boundary-based method, namely surface charge simulation method (SCSM), which is well-suited for the current work, is employed. Currently, 2D axisymmetric computer codes have been developed. Using the same, the contours of field reduction electrodes have been designed and developed to be fixed near the pin region of the insulator. The authors have developed a novel field reduction electrode both for normal and anti-fog-type disc insulator, field reduction electrode when used with insulator improve the flashover strength of ceramic/porcelain disc insulators/insulator strings significantly under polluted conditions. The field reduction element/electrode is developed to reduce the maximum field around the pin region. The method is adopted either at the time of manufacture of the insulators or for retro-fitting to the existing insulators in service. Field reduction electrode comprises of two parts: the inner electrode is made of stainless steel and the outer electrode is made of aluminum.

B. Subba Reddy and **Udaya Kumar**, HV Laboratory, Department of Electrical Engineering, Indian Institute of Science, Bangalore 560 012, India. Contact e-mail: reddy@hve.iisc.ernet.in.

2. Modeling and Simulation

In an electrostatic field, the applied excitation induces real charges on the conductor surfaces and apparent (polarization) charges on dielectric interfaces (for linear media). The resulting field distribution is equivalent to that produced by surface charge distributions on the conductor boundaries and fictitious surface charge distributions at the dielectric interfaces with dielectrics replaced by vacuum. The SCSM attempts to simulate these real and fictitious charges by piecewise-defined surface charge distributions. In other words, the SCSM involves discretization of conductor surfaces and dielectric interfaces. As a consequence, the solution will satisfy the governing differential equation exactly, but satisfies the boundary conditions only approximately. This study employs segments with a linearly varying charge distribution for the discretization and Galerkin's method for deriving the SCSM equations (Ref 7-15).

Fig. 1 Artificial pollution experimental facility

3. Calculation of Potential and Electric Field

3.1 Potential Due to Axisymmetric Strip

The potential at (r, z) due to an axisymmetric strip with respect to infinity (Ref 8, 9) is given by:

$$V(r,z) = \frac{1}{4\pi\varepsilon_o}\int_L \rho_s r' F^*(r',z')\,dl \ldots \qquad \text{(Eq 1)}$$

where, L is length of the segment, dl is an elemental length on the segment, ε_0 is the permittivity of the free space, ρ_s is the linear surface charge density, (r, z) is the coordinates of measuring point, (r', z') is a point on the source segment, $dl = \frac{L}{2}dt$. The function F^* is given by, $F^*(r',z') = \frac{4K(m)}{(a+b)^{1/2}}$, where $a = r^2 + r'^2 + (z-z')^2, b = 2rr'$, and $K(m)$ is the Elliptical integral of first kind. The linearly varying surface charge density along the coordinates are (r', z') and (r_1, z_1), and (r_2, z_2) are the coordinates of the end points of the strip. The direct analytical integration of the above equation is impractical and hence Gaussian quadrature is employed.

3.2 Electric Field Due to Axisymmetric Strip

On the similar lines, the electric field at any point (r, z) due to an axisymmetric strip charge is given by [8, 9]

$$E(r,z) = \frac{1}{4\pi\varepsilon_0}\int_L \rho_s r' H^*(r',z')dl \ldots \qquad \text{(Eq 2)}$$

where

$$H^*(r',z') = \frac{2}{r(a+b)^{1/2}}\left[K(m) - \frac{r'^2 - r^2 + (z-z')^2}{a-b}E(m)\right] \times \hat{a}_r + \left[\frac{4(z-z')}{(a-b)(a+b)^{1/2}}E(m)\right]\hat{a}_z$$

where $E(m)$ is the elliptical integral of second kind. The normal component of the field on the segment itself is computed directly by $E_n = \frac{\rho_s}{2\varepsilon_0}$.

The above mathematical steps are written in C language along with many error checking routines. The resulting matrices are inverted in Matlab and obtained charge densities are stored. Two more C programs are run to obtain the data for the equipotential and interface potential distribution. The typical run times involved for the execution of the programs are about 2 h for single disc and 6 h for 15 discs (corresponding to a 220 kV string). The computation was carried out on an Intel Pentium 4, Win XP machine with CPU of 3 GHz and 2 GB RAM.

4. Experimental Facility

The experimental facility consists of a high-voltage source of 150 kV-2 A/100 kV-3 A/50 kV-6 A with an appropriate voltage regulator and control panel as shown in Fig. 1. The facility also includes an artificial pollution chamber of 5 m^3 consisting of special nozzles for generation of artificial rain/fog and steam, fabricated and assembled as per relevant IEC/IEEE standards.

5. Insulator Profile

For this study, Type-A cap and pine type ceramic/porcelain insulator are chosen. A schematic of the ceramic insulator disc with field reduction electrode is shown in Fig. 2. The design of cap and pin type ceramic insulator essentially consists of a malleable/ductile iron cap, malleable/forged iron pin, and a ceramic/porcelain shell. The cap and pin of the insulator is fixed to the ceramic shell with the help of a Portland cement. A bituminous coating is applied to the pin to prevent corrosion. Simulations and experimentation have been carried out on various types of ceramic disc insulators, for brevity results of one type of disc insulator for various voltage levels is presented, the dimensions of insulator currently used are: disc diameter is 255 mm, height of the disc is 145 mm, and the total creep age distance is 320 mm, respectively. Field reduction electrodes comprise of two parts: the inner electrode is made of stainless steel and the outer electrode is made of aluminum. Figure 3 shows the top and bottom view of developed field reduction electrode.

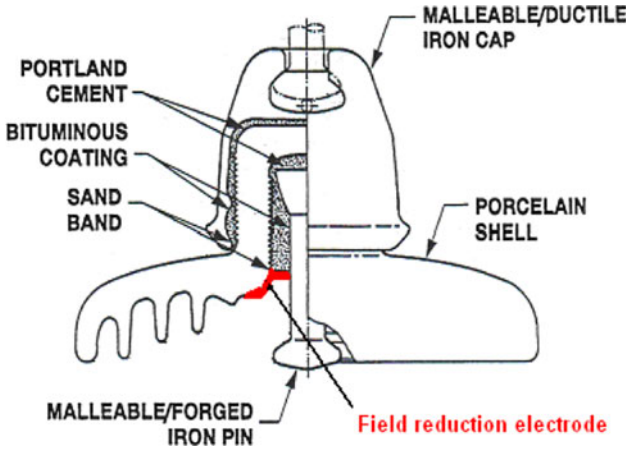

Fig. 2 Schematic of a ceramic cap and pin type insulator with field reduction electrode

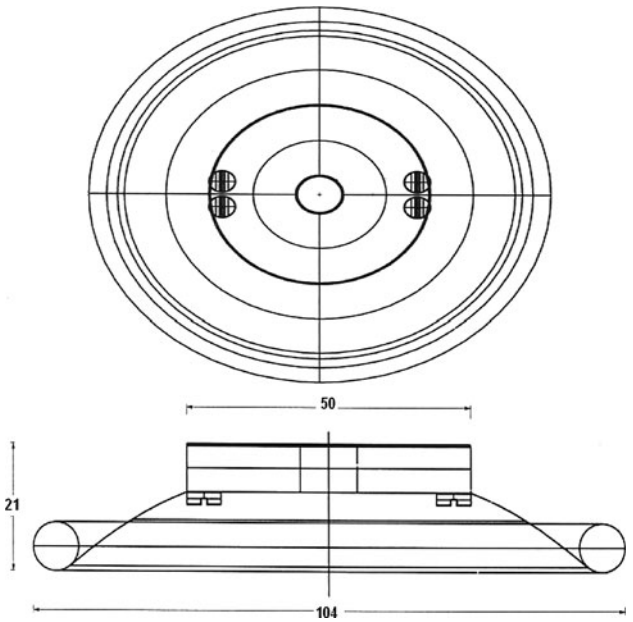

Fig. 3 Top and bottom view of field reduction electrode

6. Simulation Results

The contour plot of the potential distribution obtained for ceramic insulator Type A by the SCSM method for single disc and six discs in a string are presented in Fig. 4 and 5. The potential and tangential surface field distribution along the air insulator for single disc is shown in Fig. 6 and 7. As expected, the maximum field is very high at the pin region in comparison to the average field along the surface of the insulator. There is clearly field intensification by a factor of 6. It is worth restating here that this region has been identified as the most probable source of starting the initial scintillation/partial arcs. The results obtained for other types of insulators are on similar lines; however, for brevity they will not be presented here.

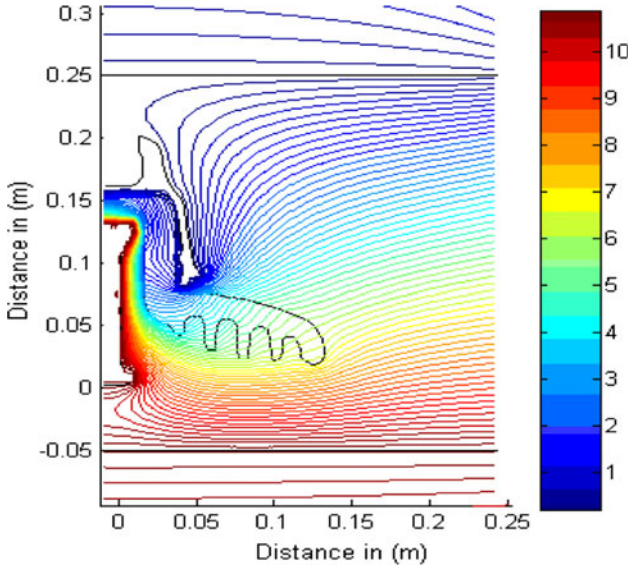

Fig. 4 Equipotential plot for type-A single disc

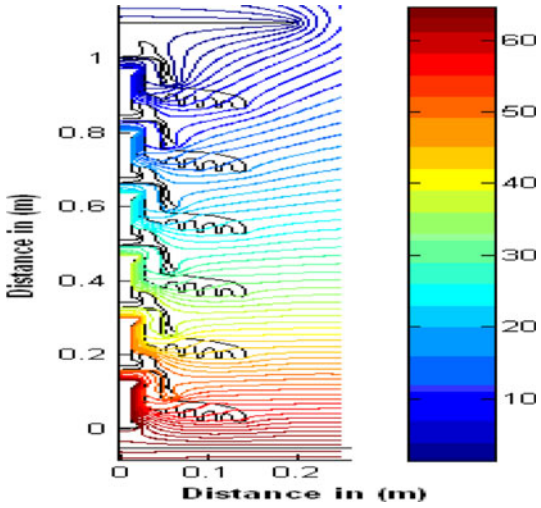

Fig. 5 Equipotential plot for a 6-disc string

After getting a clear picture on field distribution in a single disc, now analysis is extended to string of insulators with 3, 6, 9, and 14 disc strings, which correspond to 33, 66, 132, and 220 kV class, respectively. However, results corresponding to 1, 6, 9, and 14 disc string will be presented. The surface field plot along the insulator-air interface for 6, 9, and 14-disc string is shown in Fig. 8, 9, and 10, respectively.

As experienced in the laboratory tests, considerable voltage drop could be seen on the line end disc. However for the pin of the first disc and cap of the last disc, all other cap and pins form floating conductors dictating a capacitive voltage distribution. Consequently the capacitance (arising between cap and pin) of the first disc needs to carry most of the chain current which imposes a large voltage drop across it. Field plot, which is an image of potential plot, shows much larger surface field at the first disc as compared to the single disc. The simulations carried out for other type of discs showed a similar trend in potential and field distribution.

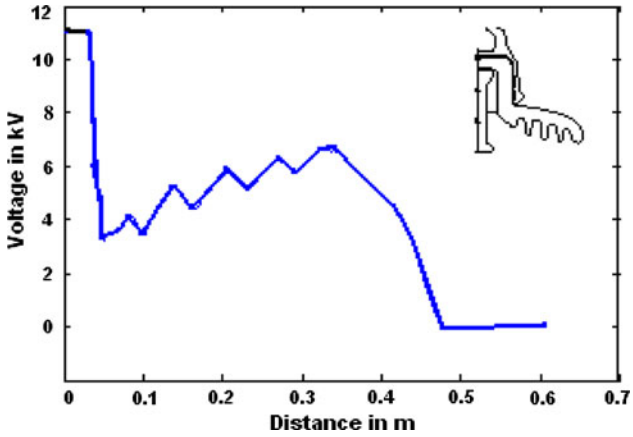

Fig. 6 Surface potential profile for single disc without electrode

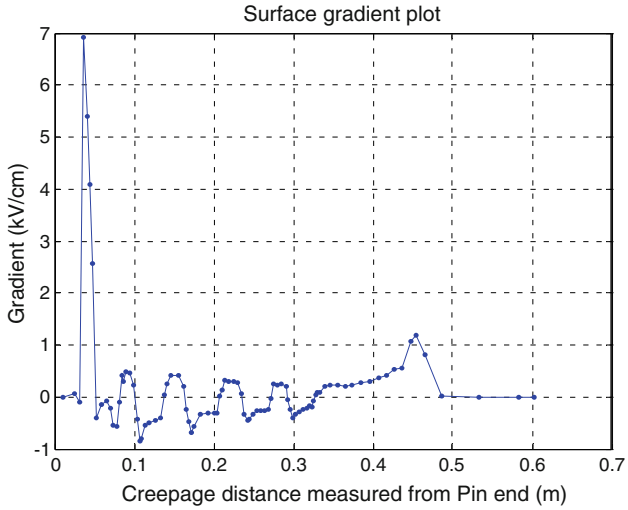

Fig. 7 Surface field for single disc without electrode

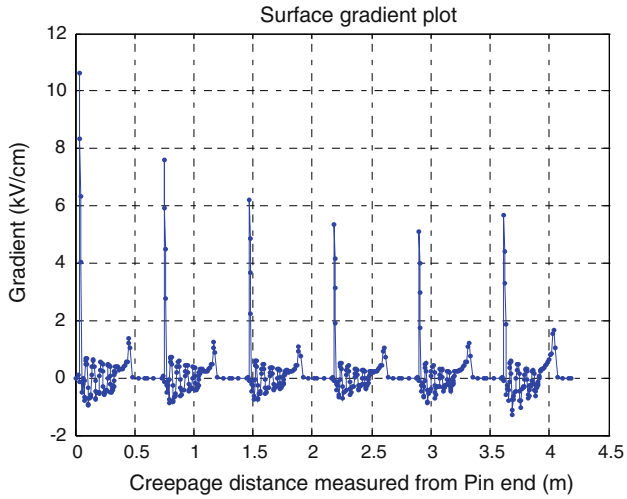

Fig. 8 Surface field for 6-disc without electrode

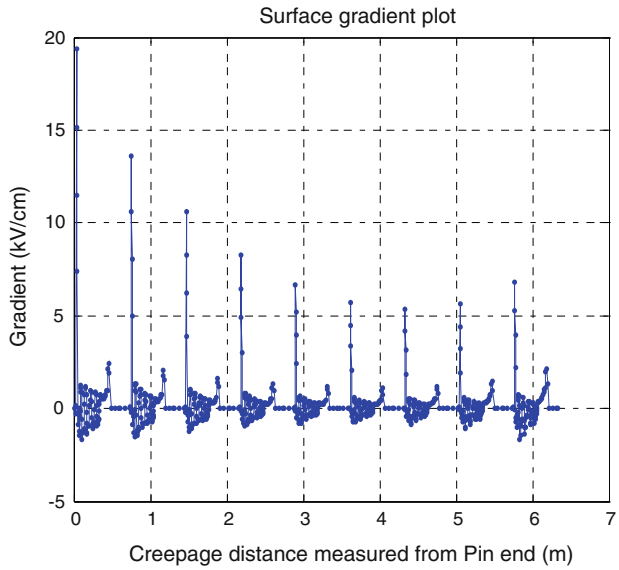

Fig. 9 Surface field for 9-disc without electrode

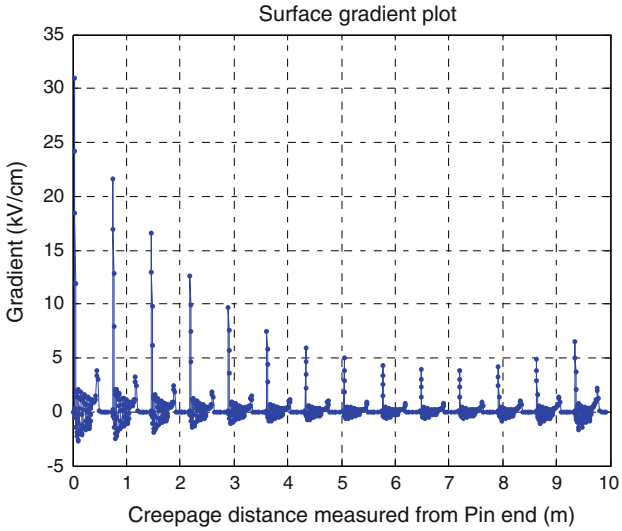

Fig. 10 Surface field for 14-disc string without electrode

As discussed in "Introduction" section, the primary objective of the present study is to reduce the maximum surface stress occurring at the pin region. Based on the field plot obtained above, a few contours for the field control electrode were arrived at and based on the pertinent study on the modified field distribution a suitable profile for the electrode was chosen. The insulators integrated with field reduction electrode are shown in Fig. 11. The simulation results for the selected field reduction electrode will be discussed below.

Yet again with field reduction electrode fixed to the insulator near the pin junction, a single disc is considered first. The surface potential and field profiles are presented in Fig. 12 and 13. By comparison with the results for normal single disc, it can be inferred that the maximum surface field is now reduced by about 40%, a significant reduction. It is worth mentioning here that the insertion of the field reduction electrode causes a sacrifice on the creepage length by only 2-3%.

Fig. 11 Three disc insulator string integrated with field reduction electrodes at the pin region

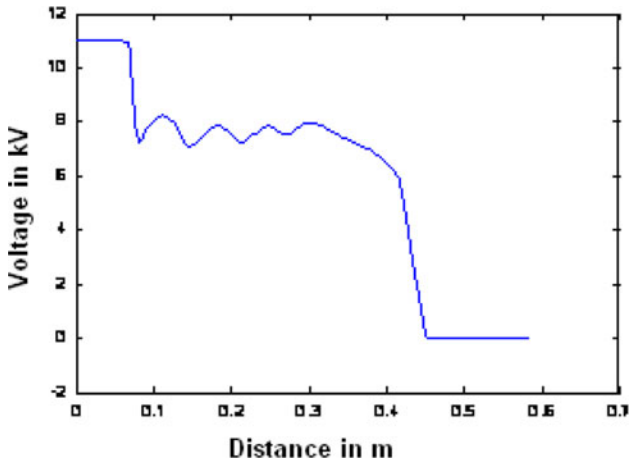

Fig. 12 Surface potential profile for single disc with electrode

Similarly, Fig. 14, 15, and 16 presents the surface field profile for 6, 9, and 14-disc string with all insulators fitted with field reduction electrode. By comparison with the string of normal discs, an overall reduction by >40% can be seen in the maximum surface field.

7. Experimentation

A preliminary set of experimentation was carried out on the same type of insulator used for simulation studies, i.e., type-A insulator disc/strings with and without field reduction electrode. Flashover strength under normal dry, wet and medium, and heavy polluted conditions as per Ref 7 is evaluated up to 132 kV class string. Even though the experiments were only preliminary, very encouraging results are obtained. Figure 17 presents the results for pollution flashover strength of a single,

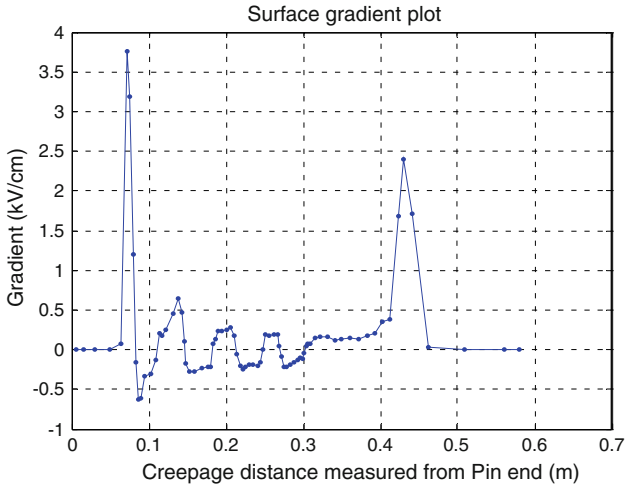

Fig. 13 Surface field for single disc with electrode

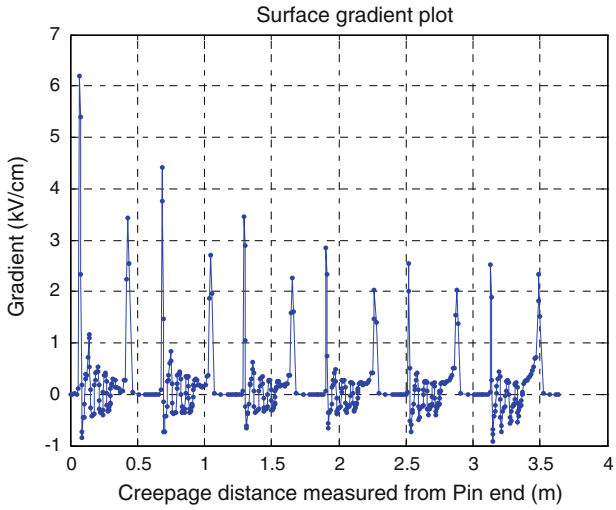

Fig. 14 Surface field for 6-disc with electrode

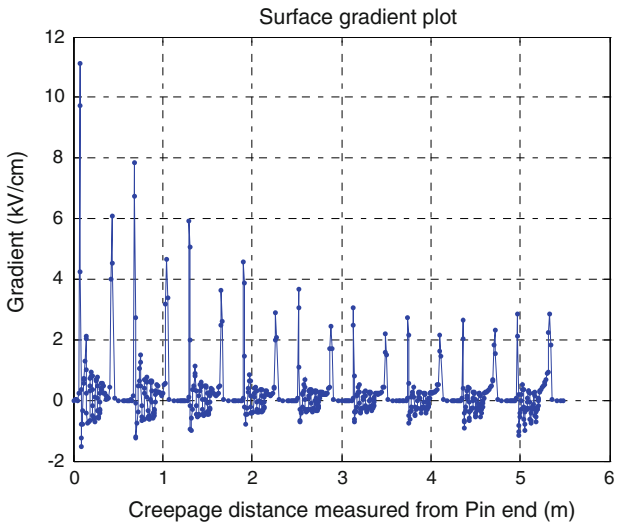

Fig. 15 Surface field for 9-disc string with electrode

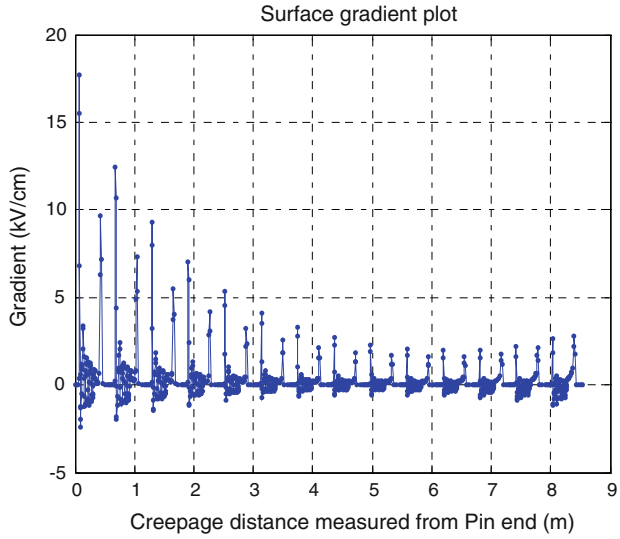

Fig. 16 Surface field for 14-disc string with electrode

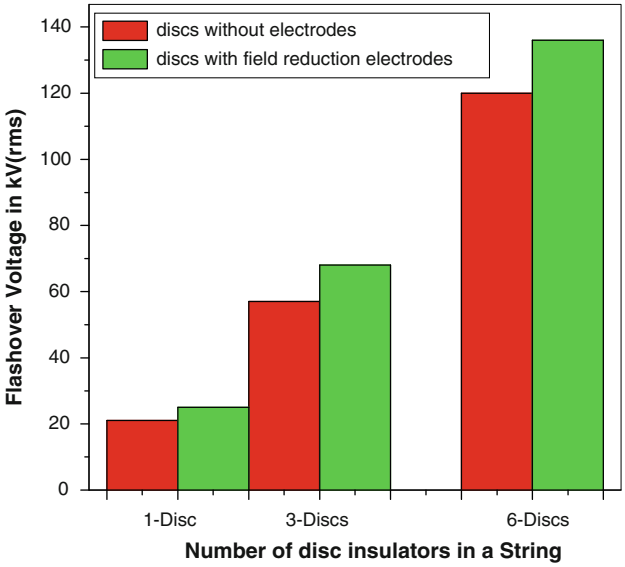

Fig. 17 Comparison of experimental results

three, and six discs in a string, the pollutants used in experimentation are 40 g of Kaolin with 5 g of NaCl per 1000 g distilled water, solid layer method as per Ref 7 was employed, results presented are the average values of 10 flashover voltages for each configuration. It is worth noting here that the improvement seems to be appreciable for the investment made (which is less than 2-3% of the cost of the insulator) on field reduction electrodes. Figures 18 and 19 show the comparison of the performance of a 6-disc insulator string without and with electrodes for the same voltage level of 28 kV (rms). It is quite clear from figures the string with field reduction electrode, i.e., Fig. 19 shows less partial arcs/scintillation activity in comparison to Fig. 18, string without electrode. This proves the influence of the developed field reduction electrode will certainly improve the pollution flashover strength of string insulators in the field.

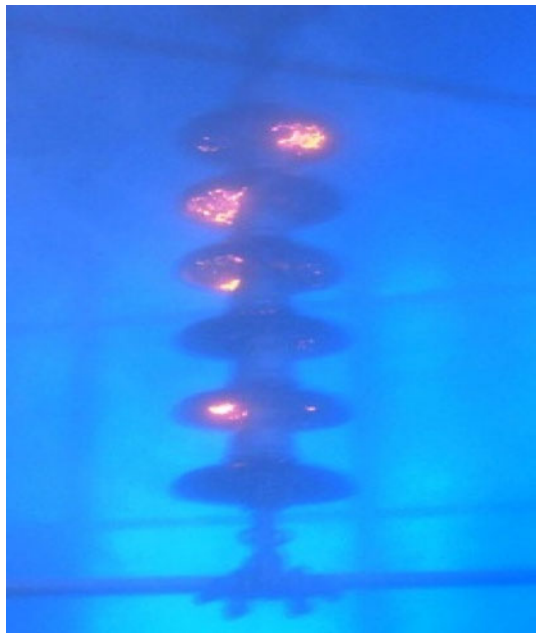

Fig. 18 Six-disc insulator string without electrodes

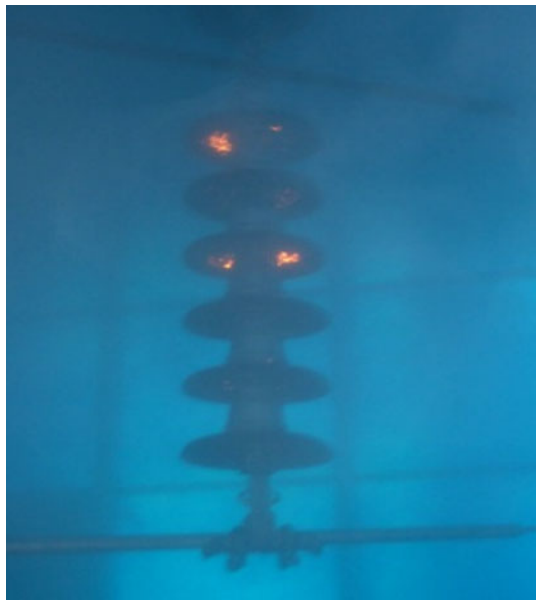

Fig. 19 Six-disc insulator string with electrodes

8. Conclusions

Performance of string insulators used in overhead power transmission lines is very critical, and it is dictated by the electric field distribution prevailing under different operating contingencies. However, a reliable electric field distribution data on commonly used disc insulators are rather sparse. Considering this, in the present study, potential and electric field profile for commonly used ceramic disc insulators are investigated.

To improve the surface flashover performance strength of the insulators during normal and polluted conditions, novel field reduction electrode is designed and developed.

Both theoretical and experimental investigations are carried out for ascertaining the improvement in the performance. Preliminary experiments carried out are in agreement with the theoretical deductions, which confirm the improvement in the performance of string insulators fitted with our field reduction electrode.

Further simulations/experimental investigations are in progress on various other types of disc insulators used in high-voltage transmission/distribution systems.

References

1. D.C. Jolly, Contamination Flashover, Part I: Theoretical Aspects, *IEEE Trans, PAS*, 1972, **PAS-91**(6), p 2437–2442
2. R. Dass, Grid Disturbance in India on 2nd January 2001, *Electra*, 2001, **196**, p 6–15
3. CEA Enquiry Committee Report of Grid Incident of Northern Region, 2007
4. CIGRE Task Force 33-04-01, Polluted Insulators: A Review of Current Knowledge, 2000
5. H. El Kishky and R.S. Gorur, Electric Potential and Field Computation Along AC HV Insulators, *IEEE Trans. DEIS*, 1994, **1**(6), p 982–990
6. S. Chakravorti and H. Steinbigler, Boundary Element Studies on Insulator Shape and Electric Field Around HV Insulators With or Without Pollution, *IEEE Trans. DEIS*, 2000, **7**(2), p 169–176
7. IEC-507-1991-04, Artificial Pollution Tests on High Voltage Insulators Used on AC Systems, 1991
8. E.H. Allen and P.L. Levin, *Two Dimensional & Axi-Symmetric Boundary Value Problems in Electrostatics*, Computational Fields Laboratory, Department of Electrical & Computer Engineering, Worcester Polytechnic Institute, Worcester, MA, 1993
9. D. Beatovic et al., A Galerkin Formulation of the Boundary Element Method for Two Dimensional and Axi-Symmetric Problems in Electrostatics, *IEEE Trans. Electr. Insulat.*, 1992, **27**(1), p 135–143
10. U. Kumar and M. Vasu, Studies on Voltage Distribution in ZnO Surge Arrester, *IEE Proc. Generat. Trans. Distrib.*, 2002, **149**(4), p 457–462
11. O.W. Andersen, Finite Element Solution of Complex Electric Fields, *IEEE Trans. PAS*, 1977, **96**(4), p 1156–1160
12. Z. Aydogmus and M. Cebeci, A New Flashover Dynamic Model of Polluted HV Insulators, *IEEE Trans. DEIS*, 2004, **11**(4), p 577–584
13. B. Subba Reddy and U. Kumar, Potential and Electric Field Profiles for Transmission Line Insulators, *4th IASTED Conference on Power & Energy Systems*, Paper no. 606-115, Langkawi, Malaysia, 2008
14. M.T. Gencoglu and M. Cebeci, The Pollution Flashover on High Voltage Insulators, *Electr. Power Syst. Res.*, 2008, **8**(11), p 1914–1921
15. B. Subba Reddy and U. Kumar, Field Reduction Electrodes for the Possible Improvement in the Pollution Flashover Performance of Porcelain Insulators, *IEEE 9th International Conference on Properties & Applications of Dielectric Materials (ICPADM-2009)* held at Harbin, China, 19th-23rd, July 2009, Vol 2, p 671–674